



Synthesis of novel epichlorohydrin cross-linked β -cyclodextrin functionalized with reduced graphene oxide composite adsorbent for treatment of phenolic wastewater

Dibya Ranjan Rout¹ · Hara Mohan Jena¹

Received: 25 February 2022 / Accepted: 18 May 2022 / Published online: 27 May 2022
© The Author(s), under exclusive licence to Springer-Verlag GmbH Germany, part of Springer Nature 2022

Abstract

A novel composite consisting reduced graphene oxide–functionalized beta-cyclodextrin epichlorohydrin polymer (RGO- β CD-ECH) was synthesized for the treatment of phenolic wastewater. Batch study of phenolic pollutants (2,4-dichlorophenol, 2-chlorophenol, and phenol) was analyzed using the synthesized composite as an adsorbent from an aqueous solution. The optimized parameters were temperature 25 °C, adsorption time 60 min, solution pH 7, and dosage 0.25 g/L. The isotherm data were more suitably fitted by the Langmuir isotherm model. The maximum uptake for 2,4-dichlorophenol, phenol, and 2-chlorophenol was 702.853, 659.475, and 674.155 mg/g, respectively, at 25 ± 1 °C. The kinetic data for all the phenolic pollutants follow the pseudo-second-order model, and the rate was controlled by film diffusion. Thermodynamic data revealed that the process of removing phenolic pollutants is spontaneous and endothermic. The composite can be used up to five cycles with a small reduction in the removal. Adsorption performance of the synthesized composite for synthetic industrial effluents shows that up to 78% removal occurred in 60 min adsorption time. Based on the remarkably rapid adsorption and high adsorption capacity, the synthesized composite can be considered an efficient adsorbent for treating phenolic pollutants from wastewater.

Keywords Epichlorohydrin · Beta-cyclodextrin · Adsorption · Langmuir · Endothermic · Wastewater

Introduction

Water pollution from anthropogenic activities and industrial operations has become a global problem due to the possible long-term hazard to human health and ecosystems. In recent times, there has been increased apprehension among scientists and researchers around the world concerning the effects of wildlife, aquatic, and human exposure to hazardous pollutants in the water system. Phenolic pollutants have been considered as the primary pollutants in surface water and groundwater due to their high toxicity, poor natural biodegradability, high oxygen demand, and long-term ecological

damages (Zhu et al. 2007). The US Environmental Protection Agency (USEPA) has listed phenolic pollutants as priority pollutants due to their bio-recalcitrant, acute toxicity nature and toxic effects on animals and human beings and stick in the aquatic environment over a very long period (Li et al. 2013). The phenolic compounds regularly enter the water bodies from domestic, agricultural, and industrial activities. Phenolic compounds like phenols and chlorophenols have been categorized as toxic phenolic pollutants.

Chlorophenols are formed by the reaction of phenols with disinfecting chlorine (Núñez-Gaytán et al. 2010). The chlorophenols like 2,4-dichlorophenol (2,4-DCP) and 2-chlorophenol (2-CP) are known as primary pollutants. These pollutants are used in paper, dyes, petrochemicals, antioxidants, plastics, wood preservatives, waste incineration, and pesticides (Jing et al. 2021). In addition, it is produced as by-products during the chlorination disinfection of drinking water as well as bleaching of pulp with chlorine. Due to the presence of chlorine groups in 2-CP and 2,4-DCP, even at low concentrations, it is very hazardous in nature in water bodies (Badu Latip et al. 2021). Phenolic pollutants

Responsible Editor: Angeles Blanco

✉ Hara Mohan Jena
hara.jena@gmail.com; hmjena@nitrkl.ac.in
Dibya Ranjan Rout
dvrout@gmail.com

¹ Department of Chemical Engineering, National Institute of Technology, Rourkela 769008, Orissa, India

possess hazardous health effects, which are both acute and chronic. Human exposure to phenol results in the irritation of the mucous membranes, eyes, and skin and affects the kidney, liver, digestive tract, lungs, and central nervous system (Anku et al. 2017; Nakhjiri et al. 2021). Even at trace concentration, its presence in surface water and groundwater causes severe health effects. Hence, there is a growing concern over the traces of phenolic levels detected in surface water and groundwater. Long-term exposure can lead to coma, tremors, muscle weakness, and irregular breathing. Chronic effects due to phenol exposure can be the dark coloration of the urine, vertigo, weight loss, anorexia, salivation, and diarrhea (Magdy et al. 2018). The allowable concentration of phenol in the surface water is less than 0.001 mg/L, and for groundwater, it is 0.0019–0.01 mg/L, according to USEPA (Kazemi et al. 2014). Therefore, cost-effective, efficient, and quick treatment methods are required to remove the phenolic contaminant from the wastewater before releasing it into the natural water body.

Various conventional techniques have been used for the treatment of phenolic pollutants from wastewater, like solvent extraction (Poonguzhali et al. 2021), chemical oxidation (Hadi et al. 2021), wet oxidation (Lal and Garg 2015), photocatalytic degradation (Landete et al. 2021), electrochemical coagulation (Olya and Pirkarami 2013), biological degradation (Hedbavna et al. 2016), ion exchange (Camacho et al. 2021), and adsorption (Feng et al. 2021; Gupta and Garg 2015). However, most of the methods have limited application due to their high cost, the longer time required to attain higher efficiency, and the production of unnecessary secondary pollutants. It is now well documented that adsorption is a promising method for wastewater treatment, as it has many advantages over other methods like high removal efficiency, cost-effectiveness, operational simplicity, design simplicity, insensitivity to toxic pollutants, application flexibility, and non-toxic end products (Xiang et al. 2021). Barring all this advantages, the adsorption process has some limitations, such as expensive adsorbent materials, difficulty in separation of pollutants from the spent adsorbents, and the deposition of spent adsorbents (Moosavi et al. 2020). Considering all the advantages and disadvantages of adsorption process, the selection of efficient adsorbents for the treatment of phenolic pollutants is of great importance. The characteristics of an efficient adsorbent are the accumulation of large quantities of pollutants on its surface, high surface area, excellent reproducibility, and fast and high desorption property and chemical stability (Efome et al. 2018). In an enormous number of studies, various adsorbents like metal oxides (Wang et al. 2018), agricultural by-products (Khenniche and Benissad-Aissani 2010), carbon nanotubes (Lee et al. 2018), activated carbon, graphene (Sahoo et al. 2020), and graphitic carbon nitride (Chegeni et al. 2019) have been explored for the effective removal of toxic environmental pollutants.

Recently, researchers have been giving much attention to synthesizing graphene-based composite adsorbents, as it will benefit various precursor materials into one adsorbent. In recent years, the application of bio-conducting polymeric composite adsorbents has gained much emphasis because of its low cost, presence of various functional groups, wide availability, and outstanding adsorption performance.

In the last decade, graphene, the new member of the carbon family, has displayed remarkable performance in wastewater treatment. It has extraordinary properties such as fast adsorption rate, abundant functional groups, good chemical stability, high surface area (2630 m²/g), and high adsorption capacity (Rout et al. 2019). However, the derivatives of graphene-like reduced graphene oxide (RGO) and graphene oxide (GO) are strongly bonded to water molecules through hydrogen and ionic bonds because of the functional groups (epoxy, hydroxyl, and carboxyl) present on the surface (Rout and Jena 2021). However, GO and RGO have specific problems like susceptibility to aggregation, surface area reduction, easy loss, low dispersion in solution, and difficulty in separation from treated wastewater (Nekouei and Nekouei 2017). Due to these specific problems, it has become a research hotspot in recent times. To overcome this, RGO is functionalized with a cross-linker (beta-cyclodextrin polymer), which attracts more attention in water treatment process.

Beta-cyclodextrin (β CD, C₄₂H₇₀O₃₅) is a truncated cone-shaped structure having seven D-glucopyranose units linked by an α -1,4-glycosidic bond (Ragavan and Rastogi 2017). It has a water-loving cavity on the external surface and a hydrophobic cavity in the center, which allows to form a host–guest inclusion complex with organic and inorganic molecules (Xu et al. 2020). Due to stable chemical structure, non-toxicity, high biodegradability, good biocompatibility, simplicity of obtainment, and porous structure, it becomes a suitable adsorbent for the adsorption of organic pollutants. However, it is a water-soluble material; as a result, its application is limited in water treatment. To overcome it, the polymerization of β CD is done with a cross-linker to make it a water-insoluble polymer. Epichlorohydrin (ECH) is chosen as a suitable cross-linker for synthesizing the insoluble polymer because of its low cost, non-toxic, and easy synthesis approach (Heydari et al. 2018).

Recently, various research activities have emphasized the synthesis of β CD and graphene-based composites for treating phenolic compounds by adsorption technique (Gholami-Bonabi et al. 2020; Gong et al. 2016; Liu et al. 2020; Wang et al. 2021). Inspired by the above research in this work, efforts have been made to synthesize RGO- β CD-ECH composite as an excellent and low-cost adsorbent for treatment of phenol, 2-CP, and 2,4-DCP from an aqueous solution in a batch study. The physicochemical properties of these three pollutants are listed in the

supporting material in Table S1. The physicochemical properties of the prepared composite were subsequently characterized using SEM, XRD, and FTIR. In addition, the effect of pH, contact time, phenolic pollutant concentration, adsorbent dosage, and temperature on the extent of adsorption of phenolic pollutants from water has been investigated. Finally, the kinetic models, isotherm models, thermodynamic parameters, desorption/regeneration, and plausible mechanism for phenolic pollutants adsorption have also been studied.

Materials and methods

Chemicals used

All materials and chemicals, which were used in this experimental section, are mentioned in supporting material section S1.

Synthesis of GO and RGO

In the modified Hummers method, NaNO_3 is replaced by H_3PO_4 and the synthesis of GO follows both oxidation and exfoliation (Smith et al. 2019). In a 1-L beaker, H_3PO_4 (30 mL) and H_2SO_4 (270 mL) were poured in ratio (1:9) and stirred for 15 min. To the above-prepared acidic solution, add 5 g of graphite powder and stir for 45 min. After that, KMnO_4 (15 g) was added slowly because of the exothermic nature of the reaction and, to maintain the temperature below 5 °C, ice bath was used. A dark green solution appeared after 6 h of vigorous stirring and then add 250 mL of DIW to the solution dropwise. Again, it was put in an ice bath to control the exothermic reaction temperature. After 15 min, add 150 mL of DIW into the solution, and the color of the solution changes to dark brown. After that, H_2O_2 (9 mL) was added to the solution and the color changed to yellowish brown. The solution was centrifuged at 8000 rpm to remove the unwanted extracts and continually bathed with DIW to make the pH of the solution 7. After that, the suspensions were put in an oven at 70 °C for 12 h to obtain the graphene oxide (GO) powder.

The procedure for reduced graphene oxide synthesis is as follows: first, the GO suspension was prepared by the addition of GO powder (1.25 g) with DIW (250 mL) and stirred for 15 min. After that, the pH was adjusted to 10 by adding HCl and NaOH solution as and when required. After that into the above solution, the reducing agent $\text{N}_2\text{H}_4\cdot\text{H}_2\text{O}$ (5 mL) was added at 65 °C and stirred for 4 h for the complete reduction. Then, the synthesized product was centrifuged and placed in an oven at 70 °C for 12 h to find RGO powder.

Synthesis of cross-linked beta-cyclodextrin epichlorohydrin polymer

The synthesis of beta-cyclodextrin epichlorohydrin ($\beta\text{CD-ECH}$) polymer occurred using ECH as a cross-linker (Gong et al. 2016). First in a beaker, add 20 mL of 50% w/w NaOH solution and βCD (10 g) was completely mixed with it and was continuously stirred for 3 h at 25 °C. ECH (6 mL) was added and stirred at 400 rpm for 40 min. Then, to stop the reaction, 15 mL acetone was added and decantation process was used to remove the excess acetone. Then, the residue was put in an oven at 50 °C for 12 h. As the above cross-linking reaction occurred in basic conditions to neutralize it, 20 mL of 6 N HCL was added. For moisture evaporation, the solution was placed at 60 °C in a dryer, and to form a white precipitate, 44 mL of ethanol was added to the solution. By decantation operation, the white precipitate was separated and put in an oven at 60 °C.

Synthesis of RGO- $\beta\text{CD-ECH}$ composite

The synthesis procedure follows first in a 1-L beaker, add 500 mL DIW, and then RGO (125 mg) was mixed by sonication. To the above solution, $\beta\text{CD-ECH}$ (2 g) was added and a homogeneous solution is formed after 30 min of stirring. Then, 5 mL of NH_4OH was added and sonicated for 60 min. Finally, a black suspension was produced, and it was constantly washed with DIW and then put in a hot air oven at 60 °C for drying.

Instrumentation

The various instruments, which are used, for the characterization of synthesized material are described in supplementary material section S2.

Batch adsorption experiments

The batch experiments were executed in a thermostatic shaker with 180-RPM speed. A total of 12.5 mg of RGO- $\beta\text{CD-ECH}$ composite was added to 50 mL of phenolic pollutant solution (100, 150, 200, 250, and 300 mg/L) under the optimized parameter conditions. The various adsorption parameters like pH = 2–10, temperature = 15–40 °C, adsorption time = 0–150 min, dosage = 5–20 mg, and initial concentration = (100–300 mg/L) were varied to find out the optimal condition for higher adsorption. HCl or NaOH solution (0.05 mol/L) was used to adjust the phenolic pollutant pH as and when required. The remaining concentrations of BPA, 2-CP, phenol, and 2,4-DCP were determined using a UV–VIS spectrophotometer (Shimadzu UV-3150 Japan) at the wavelengths of 270, 275, and 284 nm, respectively. The reusability of the RGO- $\beta\text{CD-ECH}$ composite was explored

via consecutive adsorption/desorption cycles. The uptake capacity at equilibrium (q_e) was evaluated according to the following formula:

$$q_e = \frac{(C_o - C_e) \times V}{m_s} \quad (1)$$

where V is the volume of the solution (mL), C_e and C_o (mg/L) are the equilibrium and initial phenolic pollutant concentration, and m_s (mg) is the amount of adsorbent. The removal rate was evaluated according to the following formula:

$$\%R = \frac{(C_o - C_t)}{C_o} \times 100 \quad (2)$$

Experiment with simulated effluent

As the real wastewater contains various organic and inorganic pollutants, a lab-made simulated effluent, which has similar characteristics to the textile industry and petroleum refineries industry, was used to study the effectiveness of the composite. The simulated industrial effluents consist of phenolic compounds with high salt concentrations. The composition of the simulated effluent used is as follows: phenol (100 mg/L), 2-chlorophenol (100 mg/L), 2-naphthol (20 mg/L), bisphenol A (30 mg/L), 2-nitrophenol (15 mg/L), hydroquinone (15 mg/L), potassium phosphate (30 mg/L), sodium chloride (40 mg/L), 2,4-dichlorophenol (100 mg/L), and sodium carbonate (40 mg/L). The pH of the simulated effluent was recorded as 8.2, and by adding 0.01 N HCl solution, the pH of the solution was reduced to 7. After that, 12.5 mg of RGO- β CD-ECH composite was added to the 50 mL of synthetic solution, and then, the above solution was put in a thermostatic shaker for 60 min at 30 °C. A UV–VIS spectrometer was used to measure the absorption spectra of the simulated effluent in the range of 200 to 700 nm before and after adsorption treatment. The removal percentage was calculated using the area under the absorption band.

Results and discussion

Characterization of RGO- β CD-ECH composite

SEM analysis

The surface properties and morphology of the synthesized RGO- β CD-ECH composite are studied using FESEM microscopy at different magnifications. It is observed from Fig. 1a that in GO, the sheets stuck together because of

the oxygen-containing functional groups, rough surfaces, wrinkles are present, heterogeneous surface structures, and thin sheets (Rout and Jena 2021). The FESEM image of RGO (Fig. 1b) shows the wrinkled paper-like structure, corrugated surface, less aggregate, and irregular structure (Rout and Jena 2022a, b). This change in surface properties in RGO is because of the elimination of oxygenated functional groups from GO. It can be seen from Fig. 1c that β CD-ECH polymer consists of numerous β CD units in its structure and the surface is smooth, porous in nature, has irregular solid particles, and regularly shaped, which might be due to the presence of cross-linked polymer networks. Also, these morphological properties of β CD-ECH polymer confirm that nanopore structure is not the main adsorption mechanism (Huang et al. 2018). After introducing RGO, the composite (Fig. 1d) retains the original shape and size of β CD-ECH polymer, suggesting the well-homogenized well-distributed nanolayers of RGO in the composite. Also, on the surface of the composite, many wrinkles are present and the surface is rough, indicating that β CD-ECH polymer is completely deposited onto the RGO surface.

FTIR analysis

FTIR spectra obtain the surface functional groups and chemical structural information. From our previous work, it has been observed that in GO, peaks are at 3448/cm for –OH stretching of absorbed water molecules, 1030/cm for C–O vibration, 1643/cm for C=O, 1217/cm for C–O–C vibration, and C–OH vibration at 1390/cm, which confirmed the oxidation of graphite flakes to synthesize GO (Faniyi et al. 2019). In FTIR spectra of RGO, the peak at 1560/cm is for O=C–O from carboxylate, C–O–C vibration at 1217/cm, C=C vibration at 2342/cm, and there is no hydroxyl peak around 3300–3400/cm that suggests the successful synthesis of RGO (Rout and Jena 2022a). In Fig. 2a, it is observed that in β CD-ECH polymer, lower absorption peaks are observed at 707, 756, 857, and 943/cm confirms the existence of ring vibration. The peak at 3450, 1380, 1655, and 1033/cm belongs to –OH hydroxyl group vibration, C–OH vibration, C=O carbonyl stretching, and C–O epoxide group vibration. In the FTIR spectra of the RGO-BCD-ECH composite, all the peaks of polymer and RGO are present, confirming that on the RGO surface, β CD-ECH polymers are effectively accumulated. Due to the hydrogen bonding formation between β CD-ECH and RGO, the –OH group is shifted to a lower wavenumber value (3440/cm) in the composite. In addition, the appearance of the bending vibrations of N–H for composite at 1124/cm testifies the successful introduction of amine groups in the composite.

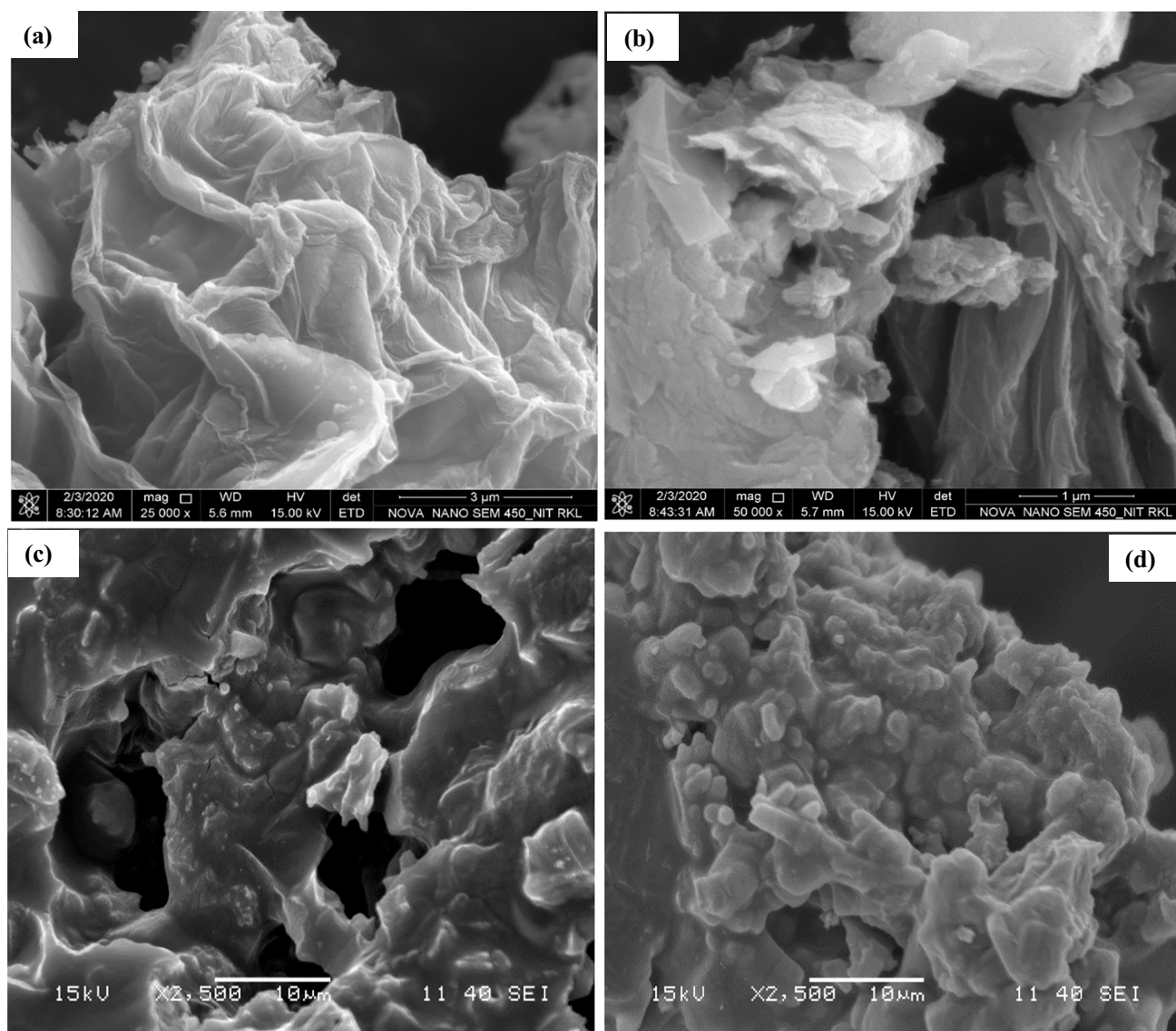


Fig. 1 FESEM image of **a** GO, **b** RGO, **c** β CD-ECH polymer and **d** RGO- β CD-ECH composite

XRD patterns

The XRD pattern of RGO- β CD-ECH composite is shown in Fig. 2b. In the XRD spectra of graphite powder, a sharp peak is obtained at a 2θ value of 26.62° with d-spacing 0.33 nm (Hidayah et al. 2017). Our previous work observed that after the introduction of oxygen functionalities, the graphitic peak shifts towards left having 2θ to a value of 12.12° ; having (001) plane for GO and d-spacing of 0.82 nm confirms the synthesis of GO (Rout and Jena 2022a). For RGO, a sharp peak is observed around 2θ value 28.68° having d-spacing 0.34 nm and (002) plane. One common peak could be seen at 41.7° (100) for both RGO and GO, which could occur due to some manganese in the synthesized GO (Rout and Jena 2022a). Two broad peaks are observed at 2θ values of 36.72°

and 53.4° in the β CD-ECH polymer (Fig. 2b) corresponding to (022) and (202) plane, which is due to the amorphous nature of the polymer (Huang et al. 2015). In the RGO- β CD-ECH composite XRD spectra, three characteristic peaks are observed at 2θ of 29.68° , 36.72° , and 53.4° , corresponding to (002), (022), and (202) plane. These peaks confirmed the successful synthesis of RGO- β CD-ECH composite.

N_2 adsorption/desorption isotherm

The textural characteristics of the RGO- β CD-ECH composite are measured by using N_2 adsorption/desorption technique. The results (Fig. 2c) displayed a type-III isotherm with type H_4 hysteresis loop associated with the co-existence of both mesoporous and microporous

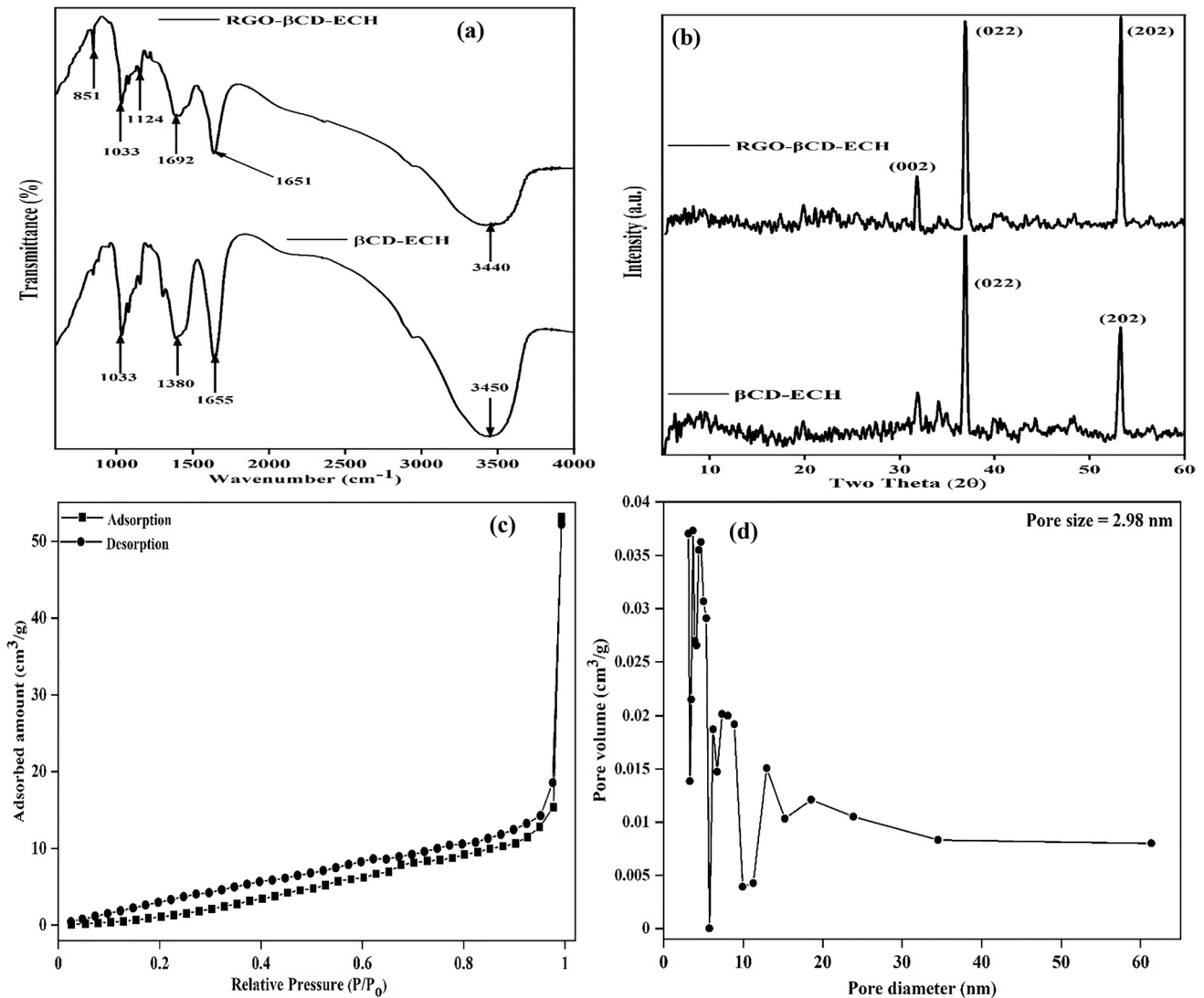


Fig. 2 a FTIR spectra, b XRD pattern, c N₂ adsorption/desorption isotherm, and d BJH pore size distribution of RGO-βCD-ECH composite

networks. The specific surface area (SSA) of the RGO-βCD-ECH composite is 35.21 m²/g which is lower than RGO (461.247 m²/g) and higher than βCD-ECH polymer (12.207 m²/g). The Barrett–Joyner–Halenda (BJH) plot (Fig. 2d) shows that sharp peaks are formed between 2.86 and 18.65 nm indicating that the synthesized RGO-βCD-ECH composite is mesoporous in nature. The pore volume of the synthesized composite is 0.085 cm³/g, whereas the mean pore diameter is 2.98 nm. After adsorption treatment, the SSA of the used RGO-βCD-ECH composite is reduced to 30.15 m²/g as some of the active sites are filled with pollutants and some pore structures collapse.

Adsorption study

Effect of solution pH

The effects of solution pH on the adsorption performance of phenolic compound (phenol, 2-CP, 2,4-DCP) using RGO-βCD-ECH composite are studied in the pH range of 2.0–10.0, at 60 min of contact time, and 15 mg of adsorbents, 100 mg/L initial phenolic compound concentration, and at room temperature (25 °C). The resulting adsorption performance is shown in Fig. 3a. It is observed

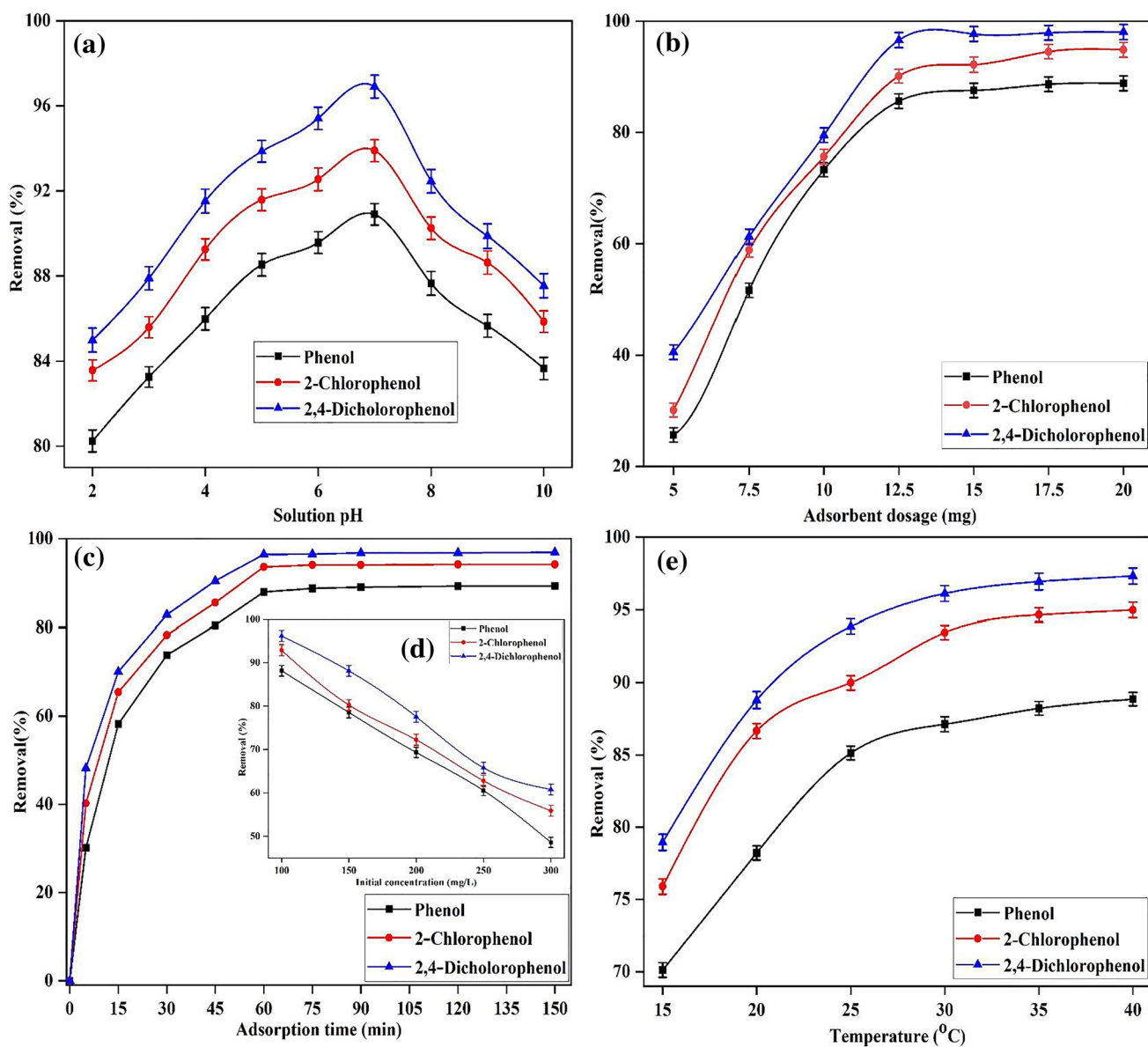


Fig. 3 Effect of **a** pH, **b** adsorbent dosage, **c** Initial concentration and contact time, and **d** temperature on phenolic pollutants removal onto RGO-βCD-ECH composite

that at both $\text{pH} < 7$ and $\text{pH} > 7$, the removal percentage decreases for all the phenolic pollutants. The maximum performances for phenol, 2-CP, and 2,4-DCP are 90.895, 93.452, and 96.745%, respectively, that occur at $\text{pH} = 7$. The pK_a values for 2,4-DCP, phenol, and 2-CP are 7.9, 9.9, and 8.8, respectively, suggesting that all phenolic compounds are weak acidic in nature (Raouf et al. 2013). Chlorophenols and phenols behave as anions at certain pH values as they are proton donors. At pH values greater than 7, the phenolic compounds became phenolate anion, and the RGO-βCD-ECH composite surface is negative ($\text{pH}_{\text{ZPC}} = 6.55$) (Rout and Jena 2022a, b) in charge; both

so repel each other as a result, and the adsorption performance decreases. In addition, at pH values greater than 7, the phenolic compounds start deprotonate and form phenolate anion as a result; the hydrogen bond between phenolic compound and adsorbent decrease causes a reduction in performance. At pH values lower than 7, the protonation of the phenolic compound starts and the H^+ ions increases in the solution. As a result, the electrostatic repulsion between protonated phenolic compounds and the H^+ ions increases and causes the depletion of the adsorption process (Zhao et al. 2021). Therefore, the pH is set at 7 for further experiments to obtain high adsorption efficiency.

Effect of adsorbent dosage

Another key parameter is the amount of adsorbent as it determines the uptake capacity for a given adsorbate concentration. The effect of composite dosage on adsorption performance is explored in the range of 5–20 mg/50 mL solution at pH of solution 7, 60 min of contact time, 100 mg/L initial phenolic compound concentration, and at room temperature (25 °C). From Fig. 3(b), it is observed that from 5 mg to 12.5 mg/50 mL, the removal of phenolic pollutants sharply increases and then attains equilibrium on the further increase. This is because as the adsorbent dosage increases, the number of available adsorption sites of the adsorbent increases. Therefore, it results in an increase in more amount of phenolic pollutants on the composite surface. However, the increment of adsorbent dosage above 12.5 mg does not allow any additional improvement in the adsorption performance. This is due to the agglomeration of phenolic pollutants on the RGO- β CD-ECH composite (Srivastava et al. 2016). Also, with an increase in dosage, equilibrium starts between unadsorbed molecules in the solution, with the molecules bonded to the adsorbent surface. As a result, the adsorbent surface becomes saturated, and the adsorption of new molecules does not occur, so the adsorption attains equilibrium. Therefore, 12.5 mg/50 mL is the optimum adsorbent dosage for further experiments to obtain high adsorption efficiency with the conditions described above.

Effect of initial phenolic pollutant concentration and adsorption time

Initial concentration of the adsorbate is one of the most important parameters of an adsorption process as it gives an essential driving force, which is required in all mass transfer operations to overcome the resistances between solid and liquid phases (Gholizadeh et al. 2013). The batch experiments were done in the concentration range of 100–300 mg/L of phenol, 2-CP, and 2,4-DCP under optimized parameter conditions at pH of solution 7, adsorption time range of 0–150 min, 12.5 mg/50 mL of adsorbent dosage, and at room temperature (25 °C). The results obtained are illustrated in Fig. 3c and d. In Fig. 3c, it has been observed that, initially, the availability of active adsorption sites are more on the surface of the adsorbent; as a result, it adsorbs more pollutants on their surface, and rapid adsorption occurs. However, with the progress of adsorption time, the active sites of the adsorbent decrease because of the agglomeration of pollutants on the adsorbent surface, so the decline rate of adsorption occurs. As the maximum adsorption occurs at 60 min of contact time for further adsorption experiments, 60 min is chosen as optimum time. Figure 3d shows that the %R decreases with an increase in initial concentration because as the initial concentration increases, it increases the mass

transfer driving force; as a result, it overcomes the mass transfer resistance between the adsorbent and adsorbate in the aqueous solution. Therefore, more adsorbate molecules start diffusing from the surface to the bulk solution, which causes a reduction in percentage removal.

Effect of temperature

The solution temperature is an essential parameter in an adsorption process, as it describes the thermodynamic state of the adsorption process. The batch adsorption experiments using RGO- β CD-ECH composite are performed from 15 to 40 °C temperature under optimized parameter conditions described above. The temperature effect on the phenolic compound removal is illustrated in Fig. 3e. The plot shows that as the temperature increases, the removal percentage also rises, suggesting the adsorption is endothermic in nature. It is observed that in up to 30 °C, the removal rate increases highly, and after that, the removal rate gradually slows down and attains equilibrium. As a result, 30 °C is chosen as the optimal temperature for further experiment. This increase in removal percentage is that with an increase in temperature, the phenolic pollutants present in solution start accelerating, leading to enhanced kinetic energy (Jiang et al. 2018). As a result, the transfer rate of phenolic ions accelerated to the surface of the composite, which enhances the adsorption performance. However, with increasing temperature, beyond 30 °C, the attractive forces between the adsorbent surface and phenolic pollutants weakened, reducing the adsorption performance.

Adsorption isotherms

The adsorption equilibrium study between the solute and solvent at a constant temperature could be analyzed by the isotherm study (Desta 2013). It is also crucial to the optimal utilization of the adsorbent. The equilibrium data of the phenolic pollutant adsorption using RGO- β CD-ECH composite are examined using Temkin, Langmuir, and Freundlich models. The surface of the adsorbent is energetically homogeneous, and the adsorption process is driven in a ratio of 1:1, where one molecule of adsorbate is bound to one binding site only (Langmuir 1918). Freundlich isotherm assumes that heterogeneous adsorption occurs in the process, where the adsorption sites are diverse and the binding sites are not saturated (Prabhakar et al. 2011). The assumption for the Temkin model is for all the molecules; adsorption heat decreases linearly rather than exponentially with an increase in amount of adsorbent. The non-linear form models could be expressed as follows (Rout and Jena 2022b):

$$q_e = \frac{q_m K_L C_e}{1 + K_L C_e} \quad (3)$$

$$q_e = k_F C_e^{1/n_F} \quad (4)$$

$$q_e = \frac{RT}{b_T} \ln(A_T C_e) \quad (5)$$

where q_m is the theoretical maximum uptake capacity of phenolic pollutant (mg/g), A_T is the binding energy (L/mg), q_e is the uptake capacity at equilibrium (mg/g), K_L (L/mg) is the affinity constant, b_T (J/mol) is the heat of adsorption,

n and K_F (mg/g)(L/mg) $^{1/n}$ are Freundlich constants, and T (K) is the temperature. The non-linear plot of the above model is displayed in Fig. 4a. Based on non-linear regression, the parameters are calculated and documented in Table 1. It is observed that for all the phenolic pollutant, the regression coefficient (R^2) and adjusted regression coefficient (R^2_{adj}) both are maximum for the Langmuir model. This confirmation indicates that the above adsorption process is monolayer adsorption. Accordingly, the q_{max} values found from the Langmuir model are 702.853, 674.155, and 659.475 mg/g, respectively, for the 2,4-DCP, 2-CP, and phenol, respectively, which are higher than that of other

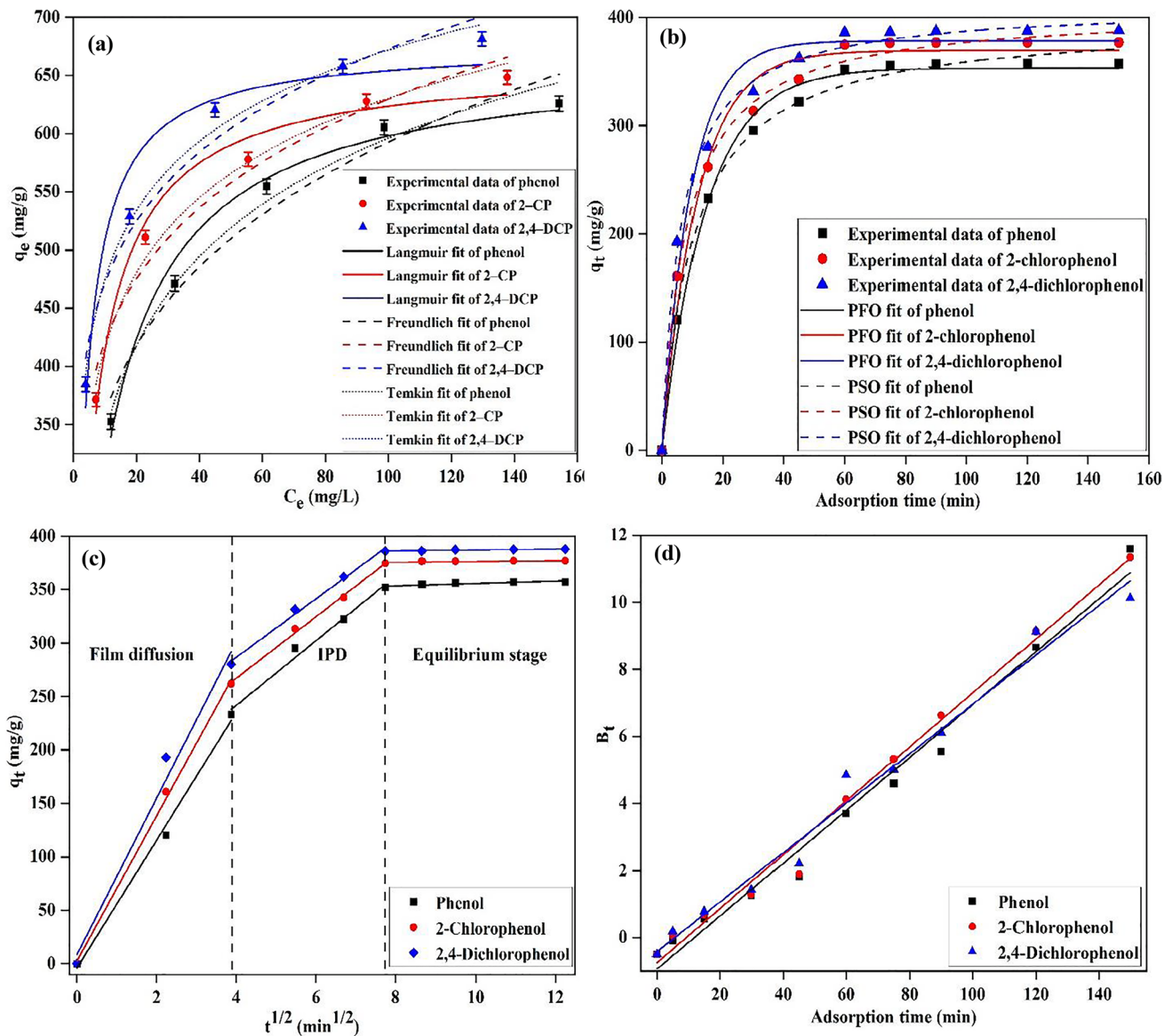


Fig. 4 a Non-linear isotherm model, b Non-linear kinetic model, c intraparticle diffusion model, and d Boyd kinetic plot for the adsorption of phenolic pollutants adsorption using RGO-βCD-ECH composite

Table 1 Langmuir, Freundlich, and Temkin isotherm parameters obtained from non-linear regression

Adsorbate	Langmuir				Freundlich				Temkin			
	q_m (mg/g)	k_L (L/mg)	R^2	R^2_{adj}	k_F (mg/g)(L/mg) ^{1/n}	1/n	R^2	R^2_{adj}	b_T (J/mol)	A_T (L/mg)	R^2	R^2_{adj}
Phenol	659.475	0.086	0.985	0.981	218.797	0.216	0.944	0.932	22.372	2.868	0.986	0.982
2-CP	674.155	0.168	0.981	0.975	280.036	0.176	0.951	0.943	26.485	5.094	0.978	0.978
2,4-DCP	702.853	0.304	0.998	0.992	326.272	0.158	0.937	0.928	28.321	8.542	0.972	0.974

Table 2 Comparison of the adsorption capacities of different adsorbents for removal of phenolic pollutants from literature

Adsorbent	Adsorption capacity(mg/g)	Conditions			Ref
		pH	Conc. (mg/L)	Temp.(K)	
Phenol					
Pomegranate peel carbon	148.380	8	50	303	Afsharnia et al. (2016)
PVAm-GO-(o-MWCNTs)-Fe ₃ O ₄	224.210	6	300	298	Zhou et al. (2020)
CNT-PEG	21.230	7	100	303	Bin-Dahman and Saleh (2020)
GO-Fe ₃ O ₄ /PRd	226.200	7	250	303	Parvin et al. (2020)
N-RGO	155.820	6	200	303	Zhao et al. (2021)
RGO-βCD-ECH composite	659.475	7	300	298	This work
2-CP					
Pristine graphene	88.100	8	100	298	Fan et al. (2017)
MRGO	63.800				Yan et al. (2016)
TNTs/ACF	122.100	5	300	295	Duan et al. (2021)
Activated biochars	150	6	300	328	Machado et al. (2020)
CCM	117.500	5	600	323	Teoh et al. (2015)
RGO-βCD-ECH composite	674.155	7	300	298	This work
2,4-DCP					
NZVI-rGO	20.120	4	20	-	Jing et al. (2021)
Fe ₃ O ₄ @AC	188.700	6	100	298	Badu Latip et al. (2021)
CS-NPC	892.860	7	500	298	Liu et al. (2021)
GN/HCP	348.430	6	500	298	Liu et al. (2020)
CSPs	848.336	6	1000	303	Zhou et al. (2019)
RGO-βCD-ECH composite	702.853	7	300	298	This work

Bold texts represent the results of this present study

adsorbents reported in the literature (Table 2) as compared to the amount of RGO-βCD-ECH composite.

Adsorption kinetic study

For any adsorption process, the mechanism involves three diffusion steps: (i) from the bulk solution, transport of the adsorbate occurs towards the film covering the adsorbent, (ii) diffusing into the adsorbent surface from the adsorbent film, and (iii) entering into the internal sites of the adsorbent and then attachment to the active sites of adsorbent (Rudzinski and Plazinski 2009). In this context, the kinetic models such as intraparticle diffusion (IPD), Elovich, pseudo-second-order (PSO), and pseudo-first-order (PFO) are widely used to interpret the experimental adsorption

data obtained from the contact time study to know the adsorption mechanism. Their equations are respectively given as follows:

$$q_t = q_e(1 - \exp^{-k_1 t}) \tag{6}$$

$$q_t = \frac{k_2 q_e^2 t}{1 + k_2 q_e t} \tag{7}$$

$$q_t = \frac{1}{\beta} \ln(1 + \alpha \beta t) \tag{8}$$

$$q_t = k_{id} t^{1/2} + C_i \tag{9}$$

where k_2 (g/mg min) is the rate constant of PSO, k_1 (/min) is the rate constants of PFO models, C_i is the boundary layer

Table 3 Parameters obtained from non-linear regression of PFO, PSO, and Elovich kinetic models for phenolic pollutant adsorption onto RGO-βCD-ECH composite

Parameters	Phenol	2-Chlorophenol	2,4-Dichlorophenol
q_{exp} (mg/g)	352.518	376.911	387.929
Pseudo-first-order			
q_{cal} (mg/g)	345.134	369.247	370.101
k_1 (/min)	0.069	0.086	0.093
R^2	0.981	0.982	0.971
ARE (%)	2.512	2.125	4.238
RMSE	8.315	7.852	16.237
Pseudo-second-order			
q_{cal} (mg/g)	354.125	379.584	393.124
$k_2 \times 10^3$ (g/mg min)	0.241	0.309	0.394
R^2	0.995	0.996	0.995
ARE (%)	1.352	0.709	1.081
RMSE	4.542	2.489	3.891

thickness, and k_{id} is the diffusion rate constant. The non-linear plots of Elovich, PFO, and PSO models are shown in Fig. 4b. The calculated and experimental values of various kinetic and statistical parameters like R^2 , RMSE, and ARE are also calculated from the non-linear plots and shown in Table 3. It is observed that PSO kinetic model is the best-fitted model for this adsorption process, which suggests that chemisorption occurs and it involves the formation of chemical bonds and electron transfer between the adsorbent and pollutant (Zhou et al. 2020).

IPD model

To know the exact diffusion mechanism in the adsorption process, the IPD model is used to identify the rate-limiting steps (Eq. 10). Figure 4c illustrates the IPD plots of phenol, 2-CP, and 2,4-DCP, and the values of C_i and k_{id} are calculated from the plot and tabulated in supporting material Table S2. Accordingly, if the plot passes the origin, then IPD is the rate-controlling step (Kumar and Jena 2016). The result indicates that the plots do not pass through the origin and three stages of straight line, revealing that IPD and some other diffusion mechanism affect the adsorption rate. The first linear part is film diffusion, where adsorbate molecules diffuse rapidly into the adsorption sites of the composite because of the availability of higher active sites. In the second part, the adsorbate molecules start diffusing into the macropores, mesopore, and micropore of composite from the surface of the adsorbent; in the final section, IPD starts to decrease. This study confirmed that the adsorption of phenolic pollutants onto the RGO-βCD-ECH composite is controlled by both film diffusion and intra-particle diffusion (Ohemeng-Boahen et al. 2021).

Boyd kinetic model

Furthermore, the exact rate-limiting steps of the process could be defined by the Boyd kinetic plot and the equation which are used are given in Eq. (10) (Liu et al. 2014).

$$B_t = -0.4977 - \ln(1 - F) \quad (10)$$

$F = q_t/q_0$ represents the fraction of phenolic pollutant and B_t is a mathematical function of F . Figure 4d shows the B_t vs. t plot for different phenol concentrations. It is observed that all the plots have y-intercept and linear, suggesting film diffusion as the rate-determining step.

Adsorption thermodynamics study

The experimental data obtained from the adsorption of phenolic pollutants (phenol, 2-CP, and 2,4-DCP) for the thermodynamic analysis on RGO-βCD-ECH composite at different temperatures (288, 293, 298, 303, 308, and 313 K) are investigated. The thermodynamics parameters are evaluated by using Eqs. (11)–(13) (Eslek Koyuncu and Okur 2021):

$$K_d = \rho \frac{q_e}{C_e} \quad (11)$$

$$\ln(K_d) = \frac{\Delta S^\circ}{R} - \frac{\Delta H^\circ}{RT} \quad (12)$$

$$\Delta G^\circ = \Delta H^\circ - T\Delta S^\circ \quad (13)$$

where ρ is the solution density (g/L) and K_d is the adsorption coefficient and a dimensionless constant. By plotting Eqs. (13), it is possible to calculate the values of ΔH° and ΔS° from the Van't Hoff plot (Fig. 5a) and the obtained ΔG° , ΔH° , and ΔS° results are presented in Table 4. It has been observed that for all the temperatures, the ΔG° values are negative for all the phenolic pollutants, which illustrate the spontaneous process that occurred. The positive value of ΔH° confirms the endothermic nature of the process, which is already discussed in the effect of temperature. The positive ΔS° values reflect the adsorbents high affinity toward phenolic pollutants and suggest that the disorder and randomness increased at the solid–liquid interface.

Reusability study

The reusability and stability of adsorbents are the most important parameters in evaluating the performance of an adsorbent as it directly relates to the cost of the adsorbent.

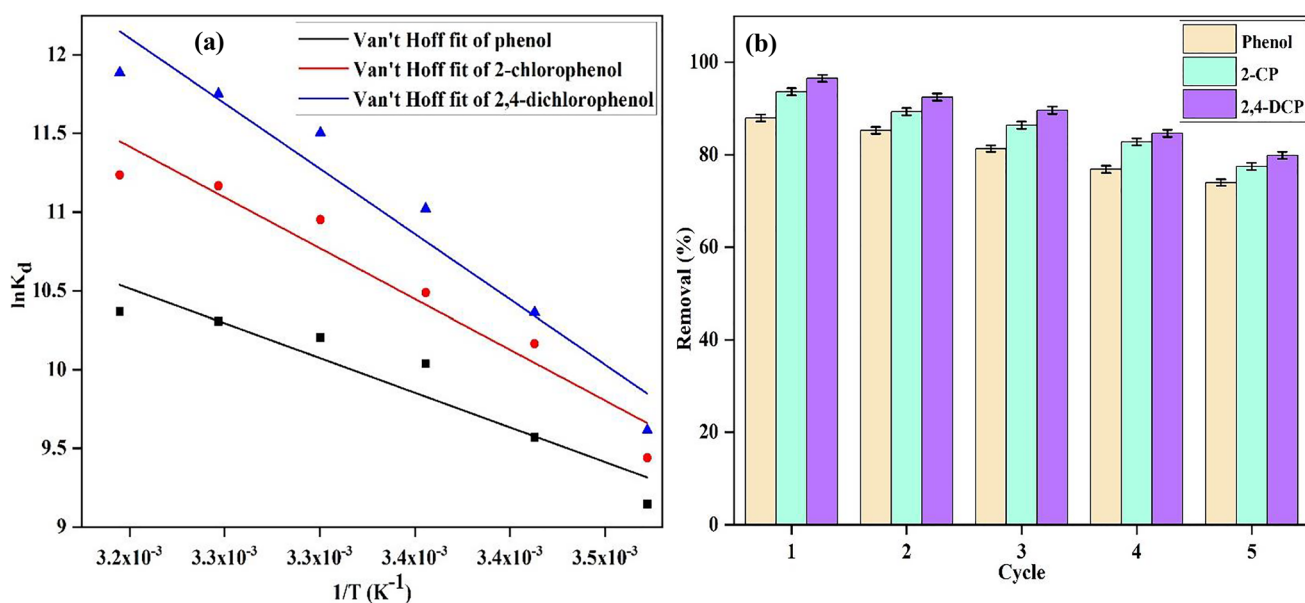


Fig. 5 **a** Van't Hoff plot and **b** regeneration study of phenolic pollutants adsorption onto RGO- β CD-ECH composite

Table 4 Estimated thermodynamic parameters

Adsorbate	Parameters	Temperature (K)					
		288	293	298	303	308	313
Phenol	ΔG° (kJ/mol)	-22.304	-23.333	-24.356	-25.381	-26.403	-27.427
	ΔH° (kJ/mol)			36.644			
	ΔS° (J/mol K)			204.682			
2-CP	ΔG° (kJ/mol)	-23.129	-24.307	-25.637	-26.967	-28.297	-29.625
	ΔH° (kJ/mol)			53.631			
	ΔS° (J/mol K)			266.53			
2,4-DCP	ΔG° (kJ/mol)	-23.418	-24.883	-26.348	-27.813	-29.278	-30.743
	ΔH° (kJ/mol)			60.966			
	ΔS° (J/mol K)			293.351			

The adsorption–desorption experiment is performed with optimal parameter conditions such as pH of solution 7, 60 min of contact time, 12.5 mg/50 mL of RGO- β CD-ECH composite dosage, and 30 °C of temperature for five consecutive cycles. After adsorption, the exhausted RGO- β CD-ECH composites are subject to regeneration by using 0.05 N HNO_3 and 0.1 M NaOH solutions as the combined eluting agents in a thermostatic shaker. After that, the regenerated adsorbents are put in an oven for drying at 60 °C for 12 h. After drying, the adsorbent is again used for the removal of pollutants with predetermined optimal conditions and this is the completion of one cycle. The same procedure follows until the completion of fifth cycle. The percentage removal of phenolic pollutants declines as cycles increase (Fig. 5b) due to the reduction of accessible active sites of the RGO- β CD-ECH composite. Furthermore, many chemical reactions occurred on the adsorbent

surface after the adsorption of phenolic pollutants, resulting in the collapse in the composite pore structure. The removal percentage of phenolic compound remained at 73.98, 77.45, and 79.85%, respectively, for phenol, 2-CP, and 2,4-DCP after five cycles of regeneration. These results indicate that the synthesized RGO- β CD-ECH composite is cost-effective and can be repeatedly applied for water purification.

Adsorption of synthetic wastewater

In industrial effluent, various types of organic and inorganic pollutants are available which is complex in nature. A simulated wastewater is prepared using various phenolic pollutants and inorganic salts to evaluate the adsorption performance of the RGO- β CD-ECH composite. The absorption

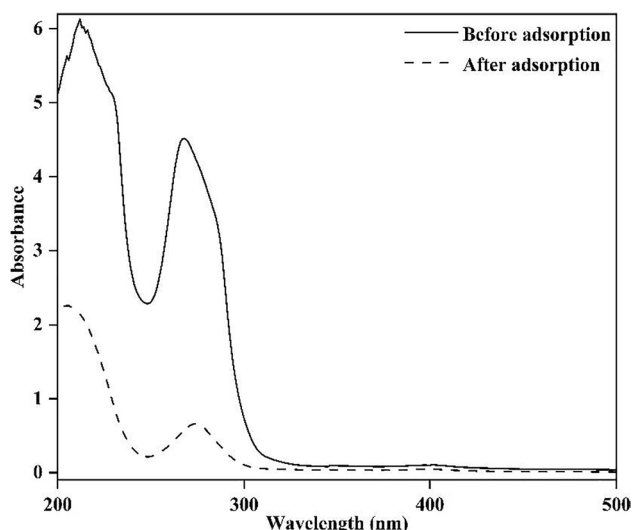


Fig. 6 UV–Vis spectra of synthetic effluent before and after adsorption using RGO- β CD-ECH composite

spectra of simulated wastewater before and after treatment are observed by using a UV–VIS spectrophotometer, and the results are shown in Fig. 6. The operating conditions for the adsorption experiments are 60 min of contact time, solution pH 7, temperature 30 °C, concentration of phenol 100 mg/L, and 12.5 mg/50 mL of adsorbent dosage. It is observed that after treatment with RGO- β CD-ECH composite, the spectra of simulated wastewater decrease and 56.14% removal percentage is achieved as compared to a single component of phenol (88.12), 2-CP (92.85), and 2,4-DCP (96.15). This decrease in removal percentage compared to the single component occurs, as in the simulated wastewater, various types of pollutants are present. All the pollutants are trying to adsorb on the adsorbent surface during adsorption. As a result, competitions among pollutants occur, resulting in decreased adsorption performance.

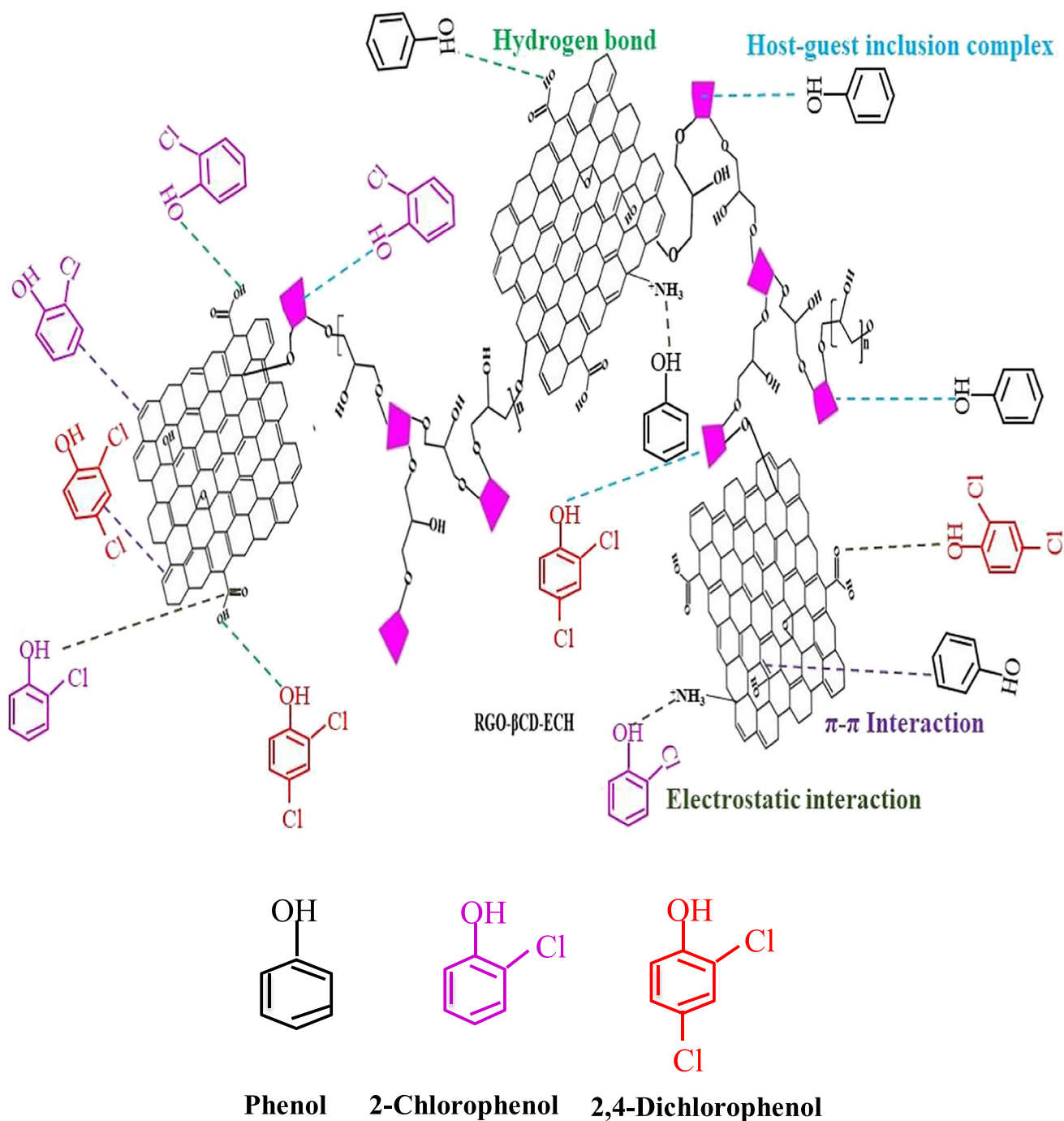
Adsorption mechanism

Several literatures reported various mechanisms for the adsorptive removal of phenolic pollutants. Out of these, the three most widely accepted mechanisms are (i) interaction of π - π electron pairing, (ii) hydrogen bond interactions, and (iii) electron donor–acceptor/electrostatic interaction. The presence of oxygen functional groups of composites at π -electron-rich regions provides complexes with aromatic rings of phenolic compounds. During the adsorption, the π -electron-rich regions of the composite act as a donor, and the phenol rings as acceptors. As a result, the adsorption of phenolic compounds onto the composite is controlled by the dispersive interaction of π - π electrons (Mojoudi et al.

2019). Adsorption on the surface of the composite is due to the formation of H bonds between the hydrogen and oxygen from the adsorbent and phenolic molecules (Dąbrowski et al. 2005). In addition, a host–guest inclusion complex is formed between β CD and phenolic compounds by Van der Waals forces and hydrogen bonds. As a result, more and more phenolic molecules are attracted towards the adsorbent surface, enhancing the adsorption process. As the reaction between phenolic molecules and the composite occurs on the entire surface of the composite, so the adsorbed phenolic molecules are uniformly distributed on the composite. In the adsorption of phenolic pollutants, two different electron donor–acceptor interaction occurs. The first one involves the interaction of carbonyl and hydroxyl groups (electron donor) of composite with the aromatic ring of phenolic compound (electron acceptor). The second one involves the interaction between amine groups (electron donor) of composite with the aromatic ring of phenolic compound (electron acceptor). The interaction between donor and acceptor of the adsorbent and phenolic compounds during the adsorption process depends on the dipole moment of the various functional groups present on the basal plane. The schematic presentation of the adsorption mechanism of phenolic compound is shown in Scheme 1.

Conclusions

The possible risk to the environment, comprising human health and aquatic resources resulting from the growing industrialization, is a real problem which needs to be addressed to remediation of phenolic compounds before it is released. This work successfully synthesized a novel composite through ECH cross-linked β CD functionalized with RGO through cross-linking reaction. The characterization study confirms the successful synthesis of our prepared composite. The batch adsorption experiments showed 88.12, 92.85, and 96.15% adsorption efficiencies for phenol, 2-CP, and 2,4-DCP, respectively, at an optimum RGO- β CD-ECH composite dosage of 0.25 g/L at pH \sim 7 at a temperature of (298 K) and time of 60 min. Langmuir model perfectly demonstrates the experimental results and the maximum uptake are 659.475, 674.155, and 702.853 mg/g, respectively, for phenol, 2-chlorophenol, and 2,4-dichlorophenol, respectively. The kinetic data follows the pseudo-second-order model, which suggests that chemisorption occurs in the adsorption process. The IPD model confirmed that three stages control the adsorption on the RGO- β CD-ECH composite. The thermodynamic study described that the adsorption of phenolic pollutants is an endothermic, favorable, and spontaneous process. In the adsorption study of simulated effluent, the novel adsorbent removes up to 56.14% of phenolic pollutants. These remarkable results concluded that the



Scheme 1 Schematic diagram for proposed phenolic compound removal mechanism.

synthesized RGO-βCD-ECH composite has great application prospect for phenolic contaminated wastewater.

Supplementary Information The online version contains supplementary material available at <https://doi.org/10.1007/s11356-022-21018-y>.

Author contribution Dibya Ranjan Rout: conceptualization; methodology; data analysis; writing—original draft preparation

Hara Mohan Jena: supervision; conceptualization; investigation; writing—review and editing.

Data availability Not applicable

Declarations

Ethics approval and consent to participate Not applicable

Consent for publication Not applicable

Competing interests The authors declare no competing interests.

References

- Afsharnia M, Saeidi M, Zarei A, Narooie MR, Biglari H (2016) Phenol removal from aqueous environment by adsorption onto pomegranate peel carbon. *Electron Physician* 8:3248–3256. <https://doi.org/10.19082/3248>
- Anku WW, Mamo MA, Govender PP (2017) Phenolic compounds in water: sources, reactivity, toxicity and treatment methods, in: Phenolic compounds - natural sources, importance and applications. InTech. <https://doi.org/10.5772/66927>
- Badu Latip NM, Gopal K, Suwaibatu M, Hashim NM, Rahim NY, Raov M, Yahaya N, Mohamad Zain NN (2021) Removal of 2,4-dichlorophenol from wastewater by an efficient adsorbent of magnetic activated carbon. *Sep Sci Technol* 56:252–265. <https://doi.org/10.1080/01496395.2020.1719156>
- Bin-Dahman OA, Saleh TA (2020) Synthesis of carbon nanotubes grafted with PEG and its efficiency for the removal of phenol from industrial wastewater. *Environ Nanotechnol Monit Manag* 13:100286. <https://doi.org/10.1016/j.enmm.2020.100286>
- Camacho MAN, López AIG, Martínez-Ferez A, Ochando-Pulido JM (2021) Two-phase olive-oil washing wastewater treatment plus phenolic fraction recovery by novel ion exchange resins process modelling and optimization. *Sep Purif Technol* 269:118755. <https://doi.org/10.1016/j.seppur.2021.118755>
- Chegeni M, Goudarzi F, Soleymani M (2019) Synthesis, characterization and application of V2O5/S-doped graphitic carbon nitride nanocomposite for removing of organic pollutants. *ChemistrySelect* 4:13736–13745. <https://doi.org/10.1002/slct.201903885>
- Dąbrowski A, Podkościelny P, Hubicki Z, Barczak M (2005) Adsorption of phenolic compounds by activated carbon—a critical review. *Chemosphere* 58:1049–1070. <https://doi.org/10.1016/j.chemosphere.2004.09.067>
- Desta MB (2013) Batch sorption experiments: Langmuir and Freundlich isotherm studies for the adsorption of textile metal ions onto teff straw (*Eragrostis tef*) agricultural waste. *J Thermodyn* 2013:1–6. <https://doi.org/10.1155/2013/375830>
- Duan J, Ji H, Xu T, Pan F, Liu X, Liu W, Zhao D (2021) Simultaneous adsorption of uranium(VI) and 2-chlorophenol by activated carbon fiber supported/modified titanate nanotubes (TNTs/ACF): effectiveness and synergistic effects. *Chem Eng J* 406:126752. <https://doi.org/10.1016/j.cej.2020.126752>
- Efome JE, Rana D, Matsuura T, Lan CQ (2018) Experiment and modeling for flux and permeate concentration of heavy metal ion in adsorptive membrane filtration using a metal-organic framework incorporated nanofibrous membrane. *Chem Eng J* 352:737–744. <https://doi.org/10.1016/j.cej.2018.07.077>
- Eslek Koyuncu DD, Okur M (2021) Removal of AV 90 dye using ordered mesoporous carbon materials prepared via nanocasting of KIT-6: adsorption isotherms, kinetics and thermodynamic analysis. *Sep Purif Technol* 257:117657. <https://doi.org/10.1016/j.seppur.2020.117657>
- Fan HT, Zhao CY, Liu S, Shen H (2017) Adsorption characteristics of chlorophenols from aqueous solution onto graphene. *J Chem Eng Data* 62:1099–1105. <https://doi.org/10.1021/acs.jced.6b00918>
- Faniyi IO, Fasakin O, Olofinjana B, Adekunle AS, Oluwasusi TV, Eleruja MA, Ajayi EOB (2019) The comparative analyses of reduced graphene oxide (RGO) prepared via green, mild and chemical approaches. *SN Appl Sci* 1:1181. <https://doi.org/10.1007/s42452-019-1188-7>
- Feng D, Guo D, Zhang Y, Sun S, Zhao Y, Shang Q, Sun H, Wu J, Tan H (2021) Functionalized construction of biochar with hierarchical pore structures and surface O-/N-containing groups for phenol adsorption. *Chem Eng J* 410:127707. <https://doi.org/10.1016/j.cej.2020.127707>
- Gholami-Bonabi L, Ziaefar N, Sheikhoie H (2020) Removal of phenol from aqueous solutions by magnetic oxide graphene nanoparticles modified with ionic liquids using the Taguchi optimization approach. *Water Sci Technol* 81:228–240. <https://doi.org/10.2166/wst.2020.082>
- Gholizadeh A, Kermani M, Gholami M, Farzadkia M, Yaghmaeian K (2013) Removal efficiency, adsorption kinetics and isotherms of phenolic compounds from aqueous solution using rice bran ash. *Asian J Chem* 25:3871–3878. <https://doi.org/10.14233/ajchem.2013.13828>
- Gong T, Zhou Y, Sun L, Liang W, Yang J, Shuang S, Dong C (2016) Effective adsorption of phenolic pollutants from water using β -cyclodextrin polymer functionalized Fe3O4 magnetic nanoparticles. *RSC Adv* 6:80955–80963. <https://doi.org/10.1039/C6RA16383A>
- Gupta A, Garg A (2015) Primary sewage sludge-derived activated carbon: characterisation and application in wastewater treatment. *Clean Technol Environ Policy* 17:1619–1631. <https://doi.org/10.1007/s10098-014-0895-4>
- Hadi S, Taheri E, Amin MM, Fatehizadeh A, Aminabhavi TM (2021) Advanced oxidation of 4-chlorophenol via combined pulsed light and sulfate radicals methods: effect of co-existing anions. *J Environ Manage* 291:112595. <https://doi.org/10.1016/j.jenvm.2021.112595>
- Hedbavna P, Rolfe SA, Huang WE, Thornton SF (2016) Biodegradation of phenolic compounds and their metabolites in contaminated groundwater using microbial fuel cells. *Bioresour Technol* 200:426–434. <https://doi.org/10.1016/j.biortech.2015.09.092>
- Heydari A, Sheibani H, Hronský V, Janigová I, Šlouf M, Šiffalovič P, Chodák I (2018) β -Cyclodextrin-epichlorohydrin polymer/graphene oxide nanocomposite: preparation and characterization. *Chem Pap* 72:1299–1313. <https://doi.org/10.1007/s11696-017-0371-9>
- Hidayah NMS, Liu W-W, Lai C-W, Noriman NZ, Khe C-S, Hashim U, Lee HC (2017) Comparison on graphite, graphene oxide and reduced graphene oxide: synthesis and characterization. In: *AIP Conference Proceedings*. 1892:150002. <https://doi.org/10.1063/1.5005764>
- Huang J, Su P, Zhao B, Yang Y (2015) Facile one-pot synthesis of β -cyclodextrin-polymer-modified Fe3O4 microspheres for stereoselective adsorption of amino acid compounds. *Anal Methods* 7:2754–2761. <https://doi.org/10.1039/C5AY00013K>
- Huang W, Hu Y, Li Y, Zhou Y, Niu D, Lei Z, Zhang Z (2018) Citric acid-crosslinked β -cyclodextrin for simultaneous removal of bisphenol A, methylene blue and copper: the roles of cavity and surface functional groups. *J Taiwan Inst Chem Eng* 82:189–197. <https://doi.org/10.1016/j.jtice.2017.11.021>
- Jiang L, Yu H-T, Pei L, Hou X (2018) The effect of temperatures on the synergistic effect between a magnetic field and functionalized graphene oxide-carbon nanotube composite for Pb 2+ and phenol adsorption. *J Nanomater* 2018:1–13. <https://doi.org/10.1155/2018/9167938>
- Jing Q, Qiao S, Xiao W, Tong L, Ren Z (2021) Efficient removal of 2,4-DCP by nano zero-valent iron-reduced graphene oxide: statistical modeling and process optimization using RSM-BBD approach. *Adsorpt Sci Technol* 2021:1–11. <https://doi.org/10.1155/2021/7130581>
- Kazemi P, Peydayesh M, Bandegi A, Mohammadi T, Bakhtiari O (2014) Stability and extraction study of phenolic wastewater treatment by supported liquid membrane using tributyl phosphate and sesame oil as liquid membrane. *Chem Eng Res Des* 92:375–383. <https://doi.org/10.1016/j.cherd.2013.07.023>

- Keshvardoostchokami M, Majidi M, Zamani A, Liu B (2021) Adsorption of phenol on environmentally friendly Fe₃O₄/chitosan/zeolitic imidazolate framework-8 nanocomposite: optimization by experimental design methodology. *J Mol Liq* 323:115064. <https://doi.org/10.1016/j.molliq.2020.115064>
- Khenniche L, Benissad-Aissani F (2010) Adsorptive removal of phenol by coffee residue activated carbon and commercial activated carbon: equilibrium, kinetics, and thermodynamics. *J Chem Eng Data* 55:4677–4686. <https://doi.org/10.1021/je100302e>
- Kumar A, Jena HM (2016) Removal of methylene blue and phenol onto prepared activated carbon from Fox nutshell by chemical activation in batch and fixed-bed column. *J Clean Prod*. <https://doi.org/10.1016/j.jclepro.2016.07.177>
- Lal K, Garg A (2015) Catalytic wet oxidation of phenol under mild operating conditions: development of reaction pathway and sludge characterization. *Clean Technol Environ Policy* 17:199–210. <https://doi.org/10.1007/s10098-014-0777-9>
- Landete JM, Rodríguez H, Curiel JA, de las Rivas B, de Felipe FL, Muñoz R (2021) Degradation of phenolic compounds found in olive products by *Lactobacillus plantarum* strains. In: *Olive and olive oil in health and disease prevention*. Elsevier 12:133–144. <https://doi.org/10.1016/B978-0-12-819528-4.00028-6>
- Langmuir I (1918) The adsorption of gases on plane surfaces of glass, mica and platinum. *J Am Chem Soc* 40:1361–1403. <https://doi.org/10.1021/ja02242a004>
- Lee KM, Wong CPP, Tan TL, Lai CW (2018) Functionalized carbon nanotubes for adsorptive removal of water pollutants. *Mater Sci Eng B* 236–237:61–69. <https://doi.org/10.1016/j.mseb.2018.12.004>
- Li Y, Jiao Y, Guo Y, Yang Y (2013) Determination of bisphenol-A, 2,4-dichlorophenol, bisphenol-AF and tetrabromobisphenol-A in liquid foods and their packaging materials by vortex-assisted supramolecular solvent microextraction/high-performance liquid chromatography. *Anal Methods* 5:5037. <https://doi.org/10.1039/c3ay40586a>
- Liu X, An S, Zhou X, Zhang L, Zhang Y, Shi W, Yang J (2014) Comparative studies of removal of methyl green and basic fuchsin from wastewater by a novel magnetic nanoparticles Mg-ferrites. *J Dispers Sci Technol* 35:1727–1736. <https://doi.org/10.1080/01932691.2013.871553>
- Liu Y, Men B, Hu A, You Q, Liao G, Wang D (2020) Facile synthesis of graphene-based hyper-cross-linked porous carbon composite with superior adsorption capability for chlorophenols. *J Environ Sci* 90:395–407. <https://doi.org/10.1016/j.jes.2019.11.018>
- Liu Y, Li L, Duan Z, You Q, Liao G, Wang D (2021) Chitosan modified nitrogen-doped porous carbon composite as a highly-efficient adsorbent for phenolic pollutants removal. *Colloids Surf A Physicochem Eng Asp* 610:125728. <https://doi.org/10.1016/j.colsurfa.2020.125728>
- Machado LMM, Lütke SF, Perondi D, Godinho M, Oliveira MLS, Collazzo GC, Dotto GL (2020) Treatment of effluents containing 2-chlorophenol by adsorption onto chemically and physically activated biochars. *J Environ Chem Eng* 8:104473. <https://doi.org/10.1016/j.jece.2020.104473>
- Magdy YM, Altaher H, ElQada E (2018) Removal of three nitrophenols from aqueous solutions by adsorption onto char ash: equilibrium and kinetic modeling. *Appl Water Sci* 8:26. <https://doi.org/10.1007/s13201-018-0666-1>
- Mojoudi N, Mirghaffari N, Soleimani M, Shariatmadari H, Belder C, Bedia J (2019) Phenol adsorption on high microporous activated carbons prepared from oily sludge: equilibrium, kinetic and thermodynamic studies. *Sci Rep* 9:19352. <https://doi.org/10.1038/s41598-019-55794-4>
- Moosavi S, Lai CW, Gan S, Zamiri G, Akbarzadeh Pivehzhani O, Johan MR (2020) Application of efficient magnetic particles and activated carbon for dye removal from wastewater. *ACS Omega* 5:20684–20697. <https://doi.org/10.1021/acsomega.0c01905>
- Nakhjiri MT, Bagheri Marandi G, Kurdtabar M (2021) Preparation of magnetic double network nanocomposite hydrogel for adsorption of phenol and p-nitrophenol from aqueous solution. *J Environ Chem Eng* 9:105039. <https://doi.org/10.1016/j.jece.2021.105039>
- Nekouei F, Nekouei S (2017) Comments on the paper “Adsorptive removal of methylene blue by rhamnolipid-functionalized graphene oxide from wastewater.” *Water Res* 108:462–463. <https://doi.org/10.1016/j.watres.2016.10.061>
- Núñez-Gaytán AM, Vera-Avila LE, De Llasera MG, Covarrubias-Herrera R (2010) Speciation and transformation pathways of chlorophenols formed from chlorination of phenol at trace level concentration. *J Environ Sci Health Part A* 45:1217–1226. <https://doi.org/10.1080/10934529.2010.493785>
- Ohemeng-Boahen G, Sewu DD, Tran HN, Woo SH (2021) Enhanced adsorption of congo red from aqueous solution using chitosan/hematite nanocomposite hydrogel capsule fabricated via anionic surfactant gelation. *Colloids Surf A Physicochem Eng Asp* 625:126911. <https://doi.org/10.1016/j.colsurfa.2021.126911>
- Olya ME, Pirkarami A (2013) Electrocoagulation for the removal of phenol and aldehyde contaminants from resin effluent. *Water Sci Technol* 68:1940–1949. <https://doi.org/10.2166/wst.2013.439>
- Parvin N, Babapoor A, Nematollahzadeh A, Mousavi SM (2020) Removal of phenol and β-naphthol from aqueous solution by decorated graphene oxide with magnetic iron for modified polyrhodanine as nanocomposite adsorbents: kinetic, equilibrium and thermodynamic studies. *React Funct Polym* 156:104718. <https://doi.org/10.1016/j.reactfunctpolym.2020.104718>
- Poonguzhali E, Kapoor A, Kumar PS, Prabhakar S (2021) Effective separation of toxic phenol from aquatic system using membranassisted solvent extraction system. *Desalin Water Treat* 221:316–327. <https://doi.org/10.5004/dwt.2021.27037>
- Prabhakar N, Matharu Z, Malhotra BD (2011) Polyaniline Langmuir-Blodgett film based aptasensor for ochratoxin A detection. *Biosens Bioelectron* 26:4006–4011. <https://doi.org/10.1016/j.bios.2011.03.014>
- Ragavan KV, Rastogi NK (2017) β-Cyclodextrin capped graphene-magnetite nanocomposite for selective adsorption of bisphenol-A. *Carbohydr Polym* 168:129–137. <https://doi.org/10.1016/j.carbpol.2017.03.045>
- Ranjan Rout D, Mohan Jena H (2022) Synthesis of novel reduced graphene oxide decorated β-cyclodextrin epichlorohydrin composite and its application for Cr(VI) removal: batch and fixed-bed studies. *Sep Purif Technol* 278:119630. <https://doi.org/10.1016/j.seppur.2021.119630>
- Raoov M, Mohamad S, Abas MR (2013) Removal of 2,4-dichlorophenol using cyclodextrin-ionic liquid polymer as a macroporous material: characterization, adsorption isotherm, kinetic study, thermodynamics. *J Hazard Mater* 263:501–516. <https://doi.org/10.1016/j.jhazmat.2013.10.003>
- Rout DR, Jena HM (2021) Removal of malachite green dye from aqueous solution using reduced graphene oxide as an adsorbent. *Mater Today Proc*. <https://doi.org/10.1016/j.matpr.2021.03.406>
- Rout DR, Jena HM (2022a) Removal of phenol from aqueous solution using reduced graphene oxide as adsorbent: isotherm, kinetic, and thermodynamic studies. *Environ Sci Pollut Res*. <https://doi.org/10.1007/s11356-021-17944-y>

- Rout DR, Jena HM (2022b) Efficient adsorption of malachite green dye using novel reduced graphene oxide/ β -cyclodextrin epichlorohydrin composite: batch and fixed-bed studies. *Int J Environ Anal Chem* 1–19. <https://doi.org/10.1080/03067319.2021.2022132>
- Rout DR, Senapati P, Sutar H, Sau DC, Murmu R (2019) Graphene oxide (GO) supported palladium (Pd) nanocomposites for enhanced hydrogenation. *Graphene* 08:33–51. <https://doi.org/10.4236/graphene.2019.83003>
- Rudzinski W, Plazinski W (2009) On the applicability of the pseudo-second order equation to represent the kinetics of adsorption at solid/solution interfaces: a theoretical analysis based on the statistical rate theory. *Adsorption* 15:181–192. <https://doi.org/10.1007/s10450-009-9167-8>
- Sahoo SK, Padhiari S, Biswal SK, Panda BB, Hota G (2020) Fe₃O₄ nanoparticles functionalized GO/g-C₃N₄ nanocomposite: an efficient magnetic nano-adsorbent for adsorptive removal of organic pollutants. *Mater Chem Phys* 244:122710. <https://doi.org/10.1016/j.matchemphys.2020.122710>
- Smith AT, LaChance AM, Zeng S, Liu B, Sun L (2019) Synthesis, properties, and applications of graphene oxide/reduced graphene oxide and their nanocomposites. *Nano Mater Sci* 1:31–47. <https://doi.org/10.1016/j.nanoms.2019.02.004>
- Srivastava SK, Senapati S, Singh SB, Raul PK (2016) Magnetic Ni/PPy nanocomposite as effective reusable adsorbent for removal of arsenite and fluoride from contaminated water. *RSC Adv* 6:113424–113431. <https://doi.org/10.1039/C6RA24531E>
- Teoh YP, Khan MA, Choong TSY, Abdullah LC, Hosseini S (2015) Comparative removal of phenols and its chlorinated derivatives by carbon-coated monolith: equilibrium, kinetics and regeneration studies. *Desalin Water Treat* 54:393–404. <https://doi.org/10.1080/19443994.2014.880378>
- Wang J, Zhang N, Jiang C, Zhang C (2018) Adsorptive removal of phenol by single and double network composite hydrogels based on hydroxypropyl cellulose and graphene oxide. *J Mater Res* 33:3898–3905. <https://doi.org/10.1557/jmr.2018.385>
- Wang H, Tian T, Wang D, Xu F, Ren W (2021) Adsorption of bisphenol A and 2,4-dichlorophenol onto cetylpyridinium chloride-modified pine sawdust: a kinetic and thermodynamic study. *Environ Sci Pollut Res*. <https://doi.org/10.1007/s11356-021-17157-3>
- Xiang L, Niu C-G, Tang N, Lv X-X, Guo H, Li Z-W, Liu H-Y, Lin L-S, Yang Y-Y, Liang C (2021) Polypyrrole coated molybdenum disulfide composites as adsorbent for enhanced removal of Cr(VI) in aqueous solutions by adsorption combined with reduction. *Chem Eng J* 408:127281. <https://doi.org/10.1016/j.cej.2020.127281>
- Xu H, Zhou C, Jian C, Yang S, Liu M, Huang X, Gao W, Wu H (2020) Salt/current-triggered stabilization of β -cyclodextrins encapsulated host-guest low-molecular-weight gels. *Chin Chem Lett* 31:369–372. <https://doi.org/10.1016/j.ccllet.2019.07.048>
- Yan H, Du Q, Yang H, Li A, Cheng R (2016) Efficient removal of chlorophenols from water with a magnetic reduced graphene oxide composite. *Sci China Chem* 59:350–359. <https://doi.org/10.1007/s11426-015-5482-y>
- Zhao R, Li Y, Ji J, Wang Q, Li G, Wu T, Zhang B (2021) Efficient removal of phenol and p-nitrophenol using nitrogen-doped reduced graphene oxide. *Colloids Surf A Physicochem Eng Asp* 611:125866. <https://doi.org/10.1016/j.colsurfa.2020.125866>
- Zhou L, Xu Z, Yi K, Huang Q, Chai K, Tong Z, Ji H (2019) Efficient remediation of 2,4-dichlorophenol from aqueous solution using B-cyclodextrin-based submicron polymeric particles. *Chem Eng J* 360:531–541. <https://doi.org/10.1016/j.cej.2018.11.196>
- Zhou K, Zhang J, Xiao Y, Zhao Z, Zhang M, Wang L, Zhang X, Zhou C (2020) High-efficiency adsorption of and competition between phenol and hydroquinone in aqueous solution on highly cationic amino-poly(vinylamine)-functionalized GO-(o-MWCNTs) magnetic nanohybrids. *Chem Eng J* 389:124223. <https://doi.org/10.1016/j.cej.2020.124223>
- Zhu X, Shi S, Wei J, Lv F, Zhao H, Kong J, He Q, Ni J (2007) Electrochemical oxidation characteristics of p-substituted phenols using a boron-doped diamond electrode. *Environ Sci Technol* 41:6541–6546. <https://doi.org/10.1021/es070955i>

Publisher's note Springer Nature remains neutral with regard to jurisdictional claims in published maps and institutional affiliations.